DOI: https://doi.org/10.67042/njss.2019.qtrrtiqp

Nigerian Journal of Soil Science

Journal homepage:www.soilsjournalnigeria.com

Geospatial predictive model for estimating soil thermal conductivity and diffusivity of Owaza gas flaring site , Southeastern Nigeria

Nwagbara, M.O.[1], Irondi, A.O., Uzoma, K.C. and Adesemuyi, E.A

Department of Soil Science and Meteorology, Michael Okpara University of Agriculture, Umudike, Abia State, Nigeria

ARTICLE INFO

Article history:

Received March, *2019*

Received in revised form July , 2019

Accepted August 10, 2019

Available online April 12, 2020

Keywords:

Gas flaring

Geospatial

Geostatistics

Kriging

Soil thermal properties

Corresponding Author's E-mail Address:

monwagbara@yahoo.com.+234806 861 1483

ISSN-1597-4488 © Publishing Realtime.

All right reserved.

ABSTRACT

In this study, predictive model for estimating the soil thermal conductivity and diffusivity from fourteen different sample points around a horizontal gas flaring site was employed in two depths (0 – 15 cm and 15 – 30 cm). Seven of these points were within the gas flare bond wall. In contrast, other points were located outside the bond wall at varying distances in the direction of the flaring. Soil temperature was determined in situ using a mercury-in-glass thermometer from these points. Core-samplers were driven into these points for dry bulk density and moisture determination. Simple descriptive statistics of mean, standard deviation and detailed geostatistics were employed to describe the variability and spatial distribution patterns of the soil thermal properties using ArcGIS 10.1. Results showed soil temperature increasing significantly (23.5 – 45 ^{o}C) as distance decreased towards the flare point. The predicted soil thermal conductivity and diffusivity values varied from 1.65 - 4.89 $Wm^{-1}K^{-1}$ and 0.77- 2.05 m^2s^{-1} within the flare bond wall and 1.58 – 1.72 $Wm^{-1}K^{-1}$ and 0.56 – 0.71 m^2s^{-1} outside the wall at 0 – 15 cm and 15 - 30 cm depths respectively. The spatial distribution maps for both soil depths showed significant variations. From the predictive soil thermal conductivity and diffusivity values, arable soil within the flare site is not suitable for agricultural activities. Therefore, for good soil health and physical characteristics, a distance of 4 km away from the flare site is recommended as soil temperature decreases with increasing distance from the site.

1.0 Introduction

Knowledge of the thermal properties of the soil top layer is of great importance in agricultural meteorology where problems of heat exchange at the soil surface are encountered. The thermal properties of soil are one of the factors that determine mass and energy exchange that takes place in the soil-plant-atmosphere system. Soil thermal properties are required to conduct analysis and modeling associated with numerous agricultural, hydrological and industrial applications. In addition to characterizing the soils physical/hydraulic properties, knowledge of the soils thermal properties is necessary for proper soil and water management in irrigated agriculture (Noborio *et al*., 1996), and in determining the energy balance at the soil surface (Hopmans and Dane, 1986). Thermal conductivity and diffusivity of soils are generally affected by soil texture and structure, increase with bulk density and moisture content, and decrease with organic matter content (Nakshabandi and Kohnke, 1965; Ghuman and Lal, 1985; Abu-Hamdeh, 2000; Abu-Hamdeh and Reeder, 2000). These soil thermal properties, especially the soil thermal diffusivity, are used in studies of soil temperature simula-

tion at different depths (Danelichen and Biudes, 2011). The soil temperature has essential biological, agricultural land climatic consequences. Indeed, soil temperatures modulate the response of many soil biological and biochemical processes (Lloyd and Taylor, 1994; Luo *et al.,* 2003). A better understanding of how different soils warm-up would benefit agriculture by allowing for better planning of planting of crops. Several authors have indicted gas flaring as the primary cause of variations in microclimate condition which have an adverse modification to climatic parameters like air and soil temperatures of the flare site, relative humidity, soil moisture and other soil properties affecting plant growth and agricultural yield (Odjugo and Osemwenkhae, 2009). It has been observed that thermal pollution from gas flares affect the microbial populations, which participate in organic matter decomposition. Almost no vegetation can grow in the area directly surrounding the flare due to the prevailing heat (Benka-Coker and Ekundayo, 1997; Boden and Andres, 2005). There is a paucity of reported work on the geospatial analysis of soil thermal properties of soils within the vicinity of a horizontal gas flaring site in Owaza, southeast Nigeria. Hence, the need for this work as knowledge of these properties is crutial since they have implications to the physical, thermal and fertility status of surrounding arable soils of the area and subsequently, the agricultural potential. This study is desirable particularly with the continuous gas flaring associated with oil exploration activities in the region. The surrounding soil is the closest contact in which these gas pipes operate especially the ground-level system (horizontal gas flaring) typical in the study area. Based on the foregoing, this study estimates soil thermal conductivity and diffusivity at Owaza horizontal gas flaring site in Abia State, Southeastern Nigeria using geostatistics.

2. Materials and Methods

2.1 Site location and characteristics

The field study was carried out within the vicinity of a horizontal gas flaring site of Shell BP gas flow station in Owaza, southeast Nigeria. The area is located within latitude 4^{o} 55' 40" N and longitude 7^{o} 10' 55" E (Figure 1). The sample points were located *in situ* at varying distances inside and outside the bond wall of the horizontal gas flaring station where spatial variability was predictable due to the apparent variable soil characteristics as a result of the gas flare heat emission within the flare bond wall and the vicinity arable soils outside the bond wall. Farming is the main socio-economic activity of the rural population with the growing of cassava (*Manihot esculenta*), maize (*Zea mays*), Fluted pumpkin (*Telfairia occidentalis*), etc in small plots at varying kilometres away from the flare site. Oil exploration started in the area in the early '60s with its resultant gas flaring. The geological material of the soil is coastal plain sand (Benin Formation) with low land geomorphology of 50 m above sea level (Enwezor *et al*., 1990). The dominant soil is described as Typic Paleudult ranging from sandy to loamy textures (USDA Soil Survey Staff, 2003). The area is warm and humid. Isohyperthermic soil temperature and udic moisture regimes characterized the area (Chukwu, 2007). There are two distinct seasons in the study area, the dry and rainy season. These seasons are usually influenced by the tropical maritime air mass and the tropical continental air mass. The rainy season usually begins in March and is interrupted by a dry season in October. Annual rainfall ranged from 2000 – 2500 mm with a mean temperature of 28 – 30^{o}C and relative humidity ranging from 55 – 85 %.

2.2 Field studies and sample collection

A field reconnaissance survey was first carried out to ascertain the feasibility of the study and appropriate clarifications were given by the host community and Shell BP Oil Servicing Company before the several field trips to the gas flare site. The study was carried out in September 2016 when the soil was wet, representing typical udic moisture regime. All data were taken when the horizontal gas flare station was actively flaring during noon between 1.00 to 3.00 pm local time, i.e. 13.00 to 15.00 Hours, GMT + 1. Sampling procedure involved the use of a fibrous measuring tape (from the active point of the horizontal gas flaring jet), to mark out sample distance points at 50 m, 100 m, 200 m distances parallel to the active flaring point (sample points 1, 2 and 3), 50 m apiece distance to the left and right sides from the active flare point (sample points 4 and 5). Sample points 6 and 7 were taken behind the active gas flaring point at 50 m and 100 m respectively all within the bond wall of the gas flaring site. In contrast, other sample points (sample points 8 through 14), were located outside the bond wall of the active flare point at varying distances (400 m, 600 m, 800 m, 1 km, 2 km, 3 km and 4 km) away from the active gas flaring point. These distances were taken to observe better the spatial scale variations of predicted soil thermal conductivities of the soils. All sample points were geo-referenced using a hand-held BHCnav GPS and their coordinates generated for further geostatistical spatial analysis using kriging.

All data were collected at 0 – 15 cm and 15 – 30 cm sampling depths from each marked sample distance point. These depths were chosen because they represent the moisture control section in the soil (USDA Soil Survey Staff, 2003). Also, these depths form the central root zone of most crops (Jang, 2004). Soil temperature was estimated in situ using a different mercury-in-glass thermometer at each sample point. Soil temperature data estimation involves immersing the bulb of the mercury thermometer 2-3 cm into 0 – 15 cm and 15 – 30 cm soil depths for five minutes each and readings (in degree Celsius) taken appropriately. Bulked soil samples from every sample point were collected using a cylindrical core sampler 3.5 cm in diameter and 6 cm in length. This involved driving the core samplers into the soil to collect undisturbed samples for soil moisture and bulk density determination. Disturbed samples were also collected from these points in three replicates for analysis of selected physicochemical properties of the soil using a handheld auger. A total of twenty-eight (28) soil samples from both sampling depths (0 – 15 cm and 15 – 30 cm) were collected for analysis of selected properties. All samples were bagged in a black polythene bag and properly labelled against each point.

2.3 Laboratory analysis

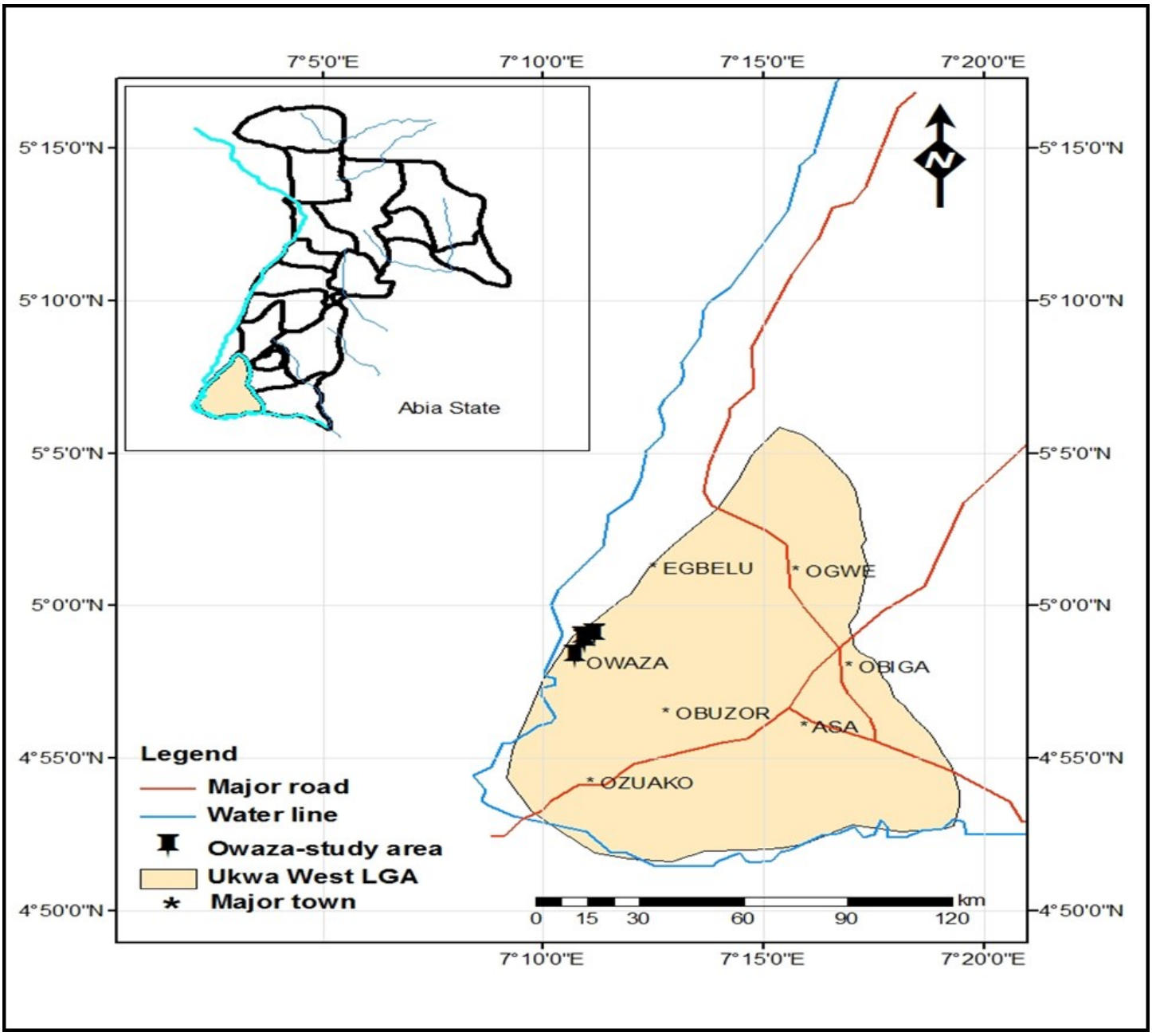


Figure 1: Map showing the location of the gas flares point in the study area

Samples were air-dried, ground, and sieved through a 2 mm screen before analyses. Prepared samples were subjected to various analysis using standard procedures as described in the USDA Soil Survey Staff (2003) at Soil Physics Laboratory of the National Root Crop Research Institute (NRCRI), Umudike, Umuahia, Abia State, Nigeria. Particle size analysis was determined using the pipette method (Gee and Or, 2002). Bulk density was analyzed by the core sample method, according to Blake and Hartage (1990) and gravimetric moisture content by the APHA (1985) method. Total porosity was calculated from the result of bulk density and particle density. Soil organic carbon was determined by the method of wet oxidation, according to Nelson and Sommers (1982).

2.4 Determination of soil thermal properties

Soil thermal conductivity

Predicted soil thermal conductivities of the soil samples were estimated using the procedure of Campbell (1985) model following the example of Ekwue *et al.* (2005, 2006, and 2011). Parameter data were translated using pedotransfer function of easily measured soil properties according to Bouma (1989). Soil dry bulk density, moisture content and percentage clay determined from the laboratory analysis were parameters inserted into the model equation. Using the Campbell (1985) model, the predicted soil thermal conductivities from different sample points were empirically determined using the model equation:

$$K = A + B\,\theta_v - (A - D)\exp\left[-(C\,\theta_v)^E\right] \quad (1)$$

Where:

K = Soil thermal conductivity (W m^{-1} $^oC^{-1}$),

Θv = Volumetric water content

ρb = Soil dry bulk density (Mg m^{-3})

Mc = Clay mass fraction from particle size analysis.

A, B, C, D and E are Soil dependent coefficients which are related to soil properties and are readily available. Campbell (1985) gave the values of the coefficients as:

$A = 0.65 - 0.78\ \rho b^{2.5}$

$B = 1.06\ \rho b^{\theta v}$

$C = 1 + 2.6\ Mc^{-0.5}$

$D = 1 + 0.03 + 0.10\ \rho b$

$E = 4$

2.4.2 Soil thermal diffusivity

The thermal diffusivity of all the soil samples points was determined by the ratio of thermal conductivity and volumetric heat capacity thus;

$$\alpha = \frac{\lambda}{Cv} \quad (2)$$

Where;

λ = Thermal conductivity ($Wm^{-1}K^{-1}$)

Cv = Volumetric heat capacity ($Jm^{-3}K^{-1}$)

α = Thermal diffusivity (m^2S^{-1})

2.5 Data analyses

Generated soil data were subjected to analysis of mean and standard deviation using M.S. Excel spreadsheet (2013) software package, according to Cruz (2013). Predicted soil thermal conductivity and thermal diffusivity were correlated and regressed against selected soil properties, and their simple coefficient of determinants was obtained using the procedure of Cohen *et al.* (2013). To describe the variability and spatial distribution patterns of the properties, a detailed geostatistical spatial analysis involving the use of Geographic Information System (GIS) was carried out in the Cartographic/GIS Laboratory of the Department of Geography and Environmental Management, University of Port Harcourt, Port Harcourt, Rivers State Nigeria. Kriging method was used in ArcGIS 10.1 environment to generate spatial maps of the selected soil thermal properties at 0 – 15 cm and 15 – 30 cm.

3. Results and discussion

3.1 Soil physicochemical properties

Selected physicochemical properties of the studied soils are shown in Table 1. $pH_{(water)}$, organic carbon (O.C.) ranged from 4.5 to 6.3 and 9.1 to 28.1 gkg^{-1} across the sample distances respectively. Clearly, sample distances (1 through 5) within the flare bond wall showed decrease values for pH(water) unlike sample points farther away outside the bond wall. In contrast, the O.C. values were higher at sample distances within the flare bond wall (point 1 through 5), and decrease at increasing distances away from the flare point outside the bond wall. Fig. 2c displays the variability trend between soil temperature and organic carbon. Clearly, at increased soil temperature, the organic carbon increases at decreased distance to the flare point and decreased at father distance away. This could be attributed to, among other things, the deposition of rich-carbon compounds associated with gas flaring. The low pH (water) closer the flare sample points agrees with the findings of Hewitt *et al.* (1995) and Botkin and Keller (1995) who showed that low pH around flare location could be attributed to acidic precipitation and emission of acidic oxides (Table 1). From the particle size analysis, the texture of sample points within the flare bond wall were predominantly sandy and loamy sand outside the bond wall. Sand content ranged from 773.0 to 873.5 gkg^{-1}. Silt ranged from 58.0 to 154.8 gkg^{-1} and was low at closer sample distances to the flare, with higher values away and outside the flare zone. Similarly, the clay content exhibited a similar trend like silt and ranged from 63.5 to 125.4 gkg^{-1} (Table 1, Fig. 2d). The high sand content and decrease clay amount across sample distances within the flaring point could be attributed to increased soil temperature as a result of heat radiation from the flare which could be induced dehydration of 2:1 clay minerals in the soil leading to strong interaction among the clay particles which in turn yielded less clay and more of larger particles (Arocena and Opio, 2003). Increased sand content within the flare vicinity agrees with previous research of Abu-Hamedh (2000) and Ekwue *et al.* (2005, 2006). The soil bulk density through the sample distances varied from 1.42 to 2.50 Mg/m^3 from farthest point away from the flare to the closest point. The moisture content ranged from 5.25 to 29.73 % across the sample points with lower values experienced within the flare points and higher values away. Soil temperature (S.T.) of the sample distances were high within the flare bond wall and ranged from 23.5 to 45.0 ^oC across the distance points (Table 2). The bulk density values of within the flare vicinity went up too high (above typical values), which could be attributed to the extreme compaction of the soils near the flare site as a result of prolonged and continuous flaring (over 50 years) in the area (Hassan and Koulhy, 2013). The tremendous heat and emission of toxic compounds could have resulted in soil surface sealing, hence the rare increase in bulk density values of sample points within the flare site. This is in good agreement with previous work by Botkin and Keller (1998) that increased soil temperature due to tremendous heat emission from gas flaring is the major cause of low soil moisture content within the flaring vicinity. Low soil moisture content leads to reduction in the rate of translocation of nutrients within the plant system as well as microbial activities. Also, induced flare radiation within the flare bond wall, must have raised the soil temperature (Orubu, 2002). Heat induces increase in bulk density through its influence on mineralization, caking of soil and infiltration of heavy metals. Clearly, the low moisture content and high soil temperature across sample distances around the flare zone could

be attributed to high evaporation due to the enormous heat radiation from the flare site.

Selected soil thermal properties

Considering the studied depth (0 – 30cm), the

Table 1: pH**,** OC and particle size distribution of different soil sample points at 0 – 30 cm depth

Sample Distance	$pH_{(water)}$ (%)	OC	Particle size distribution Sand	Silt	Clay	USDA Soil Textural Class
50 m	4.5 ± (0.20)	2.81 ± (0.10)	87.35 ± (1.00)	5.80 ± (0.40)	6.85 ± (0.10)	Loamy sand
100 m	4.7 ± (0.40)	2.62 ± (0.10)	87.17 ± (0.07)	6.47 ± (0.20)	6.35 ± (0.20)	Sand
200 m	4.6 ± (0.40)	2.72 ± (0.04)	86.75 ± (1.00)	6.90 ± (0.15)	6.35 ± (1.00)	Sand
50 m-R	4.8 ± (0.30)	2.58 ± (0.05)	86.60 ± (2.00)	6.15 ± (0.10)	7.25 ± (2.00)	Loamy sand
50 m-L	5.3 ± (0.50)	2.21 ± (0.03)	85.53 ± (0.61)	6.63 ± (0.20)	7.85 ± (0.13)	Loamy sand
50 m-B	5.6 ± (0.80)	1.65 ± (0.05)	83.97 ± (0.20)	7.17 ± (0.10)	8.85 ± (0.10)	Loamy sand
100 m-B	5.9 ± (0.50)	1.01 ± (0.06)	84.30 ± (0.25)	6.75 ± (0.35)	8.95 ± (0.05)	Loamy sand
400 m	6.2 ± (0.40)	1.53 ± (0.03)	84.30 ± (2.05)	6.15 ± (2.00)	8.95 ± (0.05)	Loamy sand
600 m	5.8 ± (0.60)	0.91 ± (0.10)	81.37 ± (1.53)	5.17 ± (0.05)	10.05 ± (0.04)	Loamy sand
800 m	6.1 ± (1.00)	1.22 ± (0.05)	78.73 ± (1.00)	9.80 ± (0.17)	9.98 ± (0.30)	Loamy sand
1 km	5.9 ± (1.00)	1.31 ± (0.06)	75.70 ± (0.50)	13.32 ± (0.10)	11.46 ± (1.00)	sandy loam
2 km	6.3 ± (1.00)	1.34 ± (0.04)	72.60 ± (0.30)	15.48 ± (0.20)	11.92 ± (0.20)	sandy loam
3 km	5.7 ± (1.00)	1.40 ± (0.15)	77.30 ± (0.25)	10.70 ± (0.30)	12.0 ± (2.00)	sandy loam
4 km	5.9 ± (0.75)	1.44 ± (0.10)	9.69 ± (0.10)	9.69 ± (0.10)	12.54 ± (0.10)	sandy loam

Key: 50 m-R and 50 m-L = 50 m interval distance points to the right and left from the active flare point, 50 m-B and 100 m-B = 50 m and 100 m distance points behind the active flare point, pH_{water} = pH in water, OC = Organic carbon, Values in bracket = Standard deviation. All values are means of three replicate samples.

predicted soil thermal conductivity varied from 1.58 to 4.89 $Wm^{-1} K^{-1,}$ whereas the standard deviation (S.D.) ranged from 0.06 to 0.28. The thermal diffusivity followed similar trend in variation as was observed in thermal conductivity. The mean values from sample points 1 to 14 varied from 0.56 to 2.05 m^2s^{-1}, whereas S.D. ranged from 0.05 to 0.15 (Table 2). High predicted soil thermal conductivity predominate sample points within the bond wall of the flaring site. Increased soil temperature at closer sample points and subsequent increase in soil bulk density, led to more significant contacts between soil solid particles which resulted in increased predicted soil thermal conductivity within the flare site. This agrees with the findings of Campell *et al.* (1994) and Smits *et al.* (2013) that soil thermal conductivity increases with rising temperature. Udoinyang (2005) further opined that the higher values of predicted soil thermal conductivity closer to the gas flare sample points are as a result of intense heat and higher temperatures generated by the gas flare station.

Similarly, Ikelegbe (1993) and Orubu (2002) observed that gas flaring generate tremendous heat, which is felt over an average radius of 0.5 kilometres thereby causing soil thermal pollution. Increased bulk density of soils closer to the flare point results in more intimate contact between the individual particles, and this brings about increases in thermal conductivity (Nakshabandi and Kohnke, 1965). The predicted soil thermal conductivity also increases with water content because the thickness and geometric arrangement of water layer around soil particles improve thermal contact between soil particles; hence increase in predicted soil thermal conductivity (Hillel, 1998). This is not in agreement from the result of this study as predicted soil thermal conductivity was highest across sample points with low moisture content (See Table 2). The increase in predicted soil thermal conductivity within the gas flare vicinity could be as a result of the increase in soil temperature and high bulk density due to high heat radiation. Furthermore, many authors indicted increase in bulk density and moisture content as a cause of the increase in thermal conductivity (Oladunjoye and Sanuade, 2012; Rubio *et al.,* 2009; Singh and Devid, 2000).

Similarly, the higher soil thermal diffusivity values observed within the flare bond wall could be attributed to the high heat emission from the flare resulting in increased heat transmission through the soil profile. Fig. 2a shows a variation of predicted soil thermal conductivity in studied soils with soil temperature. The predicted thermal conductivity values increased with increasing soil temperature within the flare bond wall and decreased away. Similarly, the predicted thermal diffusivity followed the same pattern of increase towards the flare (Fig. 2b). It could be observed that at increased soil temperature, the predicted soil thermal conductivity and diffusivity subsequently increased within the flare bond wall in the direction of flaring and decreases sharply and continuously away from the flare zone. This agrees with the findings of Campbell *et al.*

Table 2: Physical soil properties, soil temperatures, thermal conductivity and diffusivity of different sample points at 0 – 30cm depth

Sample Distance	BD (Mg/m^3)	GMC (%)	ST (^oC)	Predicted thermal conductivity ($Wm^{-1}K^{-1}$)	Predicted thermal diffusivity (m^2s^{-1})	Soil coordinates Latitude (N)	Longitude (E)
50 m	2.50 ± (0.06)	5.25 ± (0.50)	45.0 ± (0.50)	4.89 ± (0.19)	2.05 ± (0.07)	4°58^{1}48.67°	7°10^{1}59.79°
100 m	2.45 ±(0.05)	5.35 ±(0.65)	43.5 ± (0.30)	4.69 ± (0.27)	1.96 ± (0.06)	4°58^{1}48.28°	7°11^{1}0.79°
200 m	2.38 ±(0.05)	5.60 ±(0.60)	42.5 ± (0.40)	4.33 ± (0.10)	1.87 ± (0.15)	4°58^{1}46.98°	7°11^{1}0.34°
50 m-R	2.15 ±(0.05)	7.82 ±(1.40)	40.5 ± (0.50)	3.40 ± (0.20)	1.50 ± (0.05)	4°58^{1}46.03°	7°11^{1}0.05°
50 m-L	2.07 ±(0.14)	8.53 ±(1.10)	39.5 ± (0.50)	3.10 ± (0.09)	1.37 ± (0.07)	4°58^{1}46.09°	7°10^{1}59.17°
50 m-B	1.59 ±(0.07)	13.41 ± (1.22)	34.0 ± (0.50)	1.65 ± (0.10)	0.83 ± (0.08)	4°58^{1}49.54°	7°10^{1}57.12°
100 m	1.57 ±(0.07)	15.54 ± (2.05)	32.5 ± (0.30)	1.65 ± (0.13)	0.77 ± (0.07)	4°58^{1}52.82°	7°10^{1}58.57°
400 m	1.55 ±(0.08)	19.69 ± (2.05)	35.5 ± (0.40)	1.72 ± (0.19)	0.71 ± (0.06)	4°58^{1}56.38°	7°10^{1}58.48°
600 m	1.54 ±(0.16)	21.93 ± (2.00)	31.0 ± (2.00)	1.76 ± (0.25)	0.69 ± (0.09)	4°58^{1}58.97°	7°10^{1}57.98°
800 m	1.54 ±(0.06)	21.85 ± (2.15)	31.0 ± (0.50)	1.73 ± (0.29)	0.69 ± (0.09)	4°58^{1}56.89°	7°10^{1}56.84°
1 km	1.45 ±(0.06)	23.56 ± (1.50)	28.5 ± (1.00)	1.54 ± (0.28)	0.62 ± (0.07)	4°58^{1}53.14°	7°11^{1}02.80°
2 km	1.42 ±(0.08)	25.79 ± (1.52)	26.5 ± (1.50)	1.49 ± (0.05)	0.58 ± (0.08)	4°58^{1}57.40°	7°11^{1}14.02°
3 km	1.44 ±(0.05)	26.79 ± (0.58)	25.5 ± (1.50)	1.57 ± (0.06)	0.58 ± (0.08)	4°58^{1}57.40°	7°11^{1}14.02°
4 km	1.42 ±(0.04)	29.73 ± (2.00)	23.5 ± (0.50)	1.58 ± (0.06)	0.56 ± (0.07)	4°59106.91°	7°11^{1}12.09°

Key: 50 m-R and 50 m-L = 50 m interval distance points to the right and left from the active flare point, 50 m-B and 100 m-B = 50m and 100 m distance points behind the active flare point, BD = bulk density, GMC = gravimetric moisture content, ST = Soil temperature, values in bracket = Standard deviation. All values are means of three replicate samples

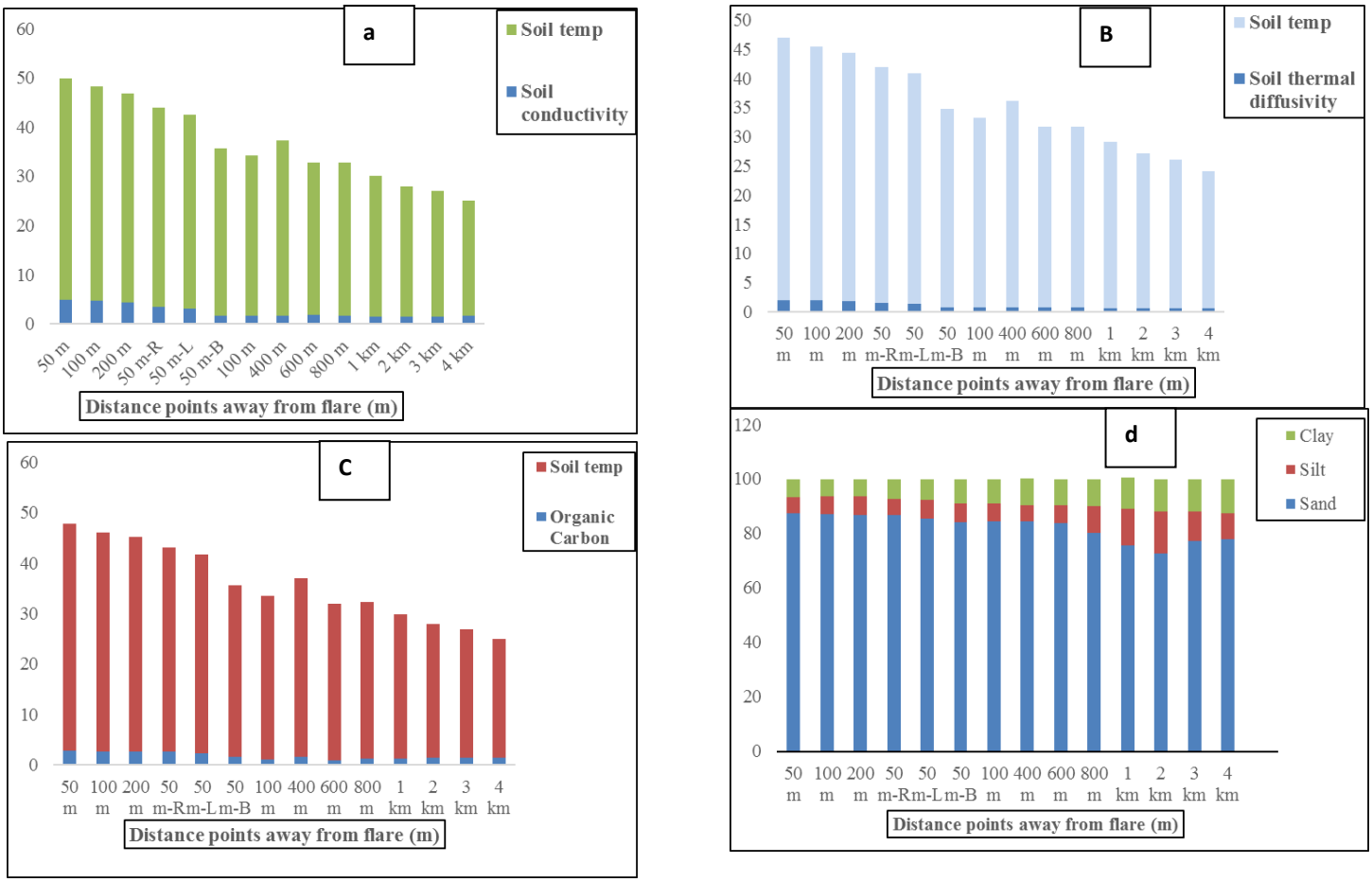


Fig 2. : Variability trend between (a) soil temperature and predicted soil thermal conductivity; (b) soil temperature and predicted soil thermal diffusivity; (c) soil temperature and organic carbon; and (d) particle size distribution

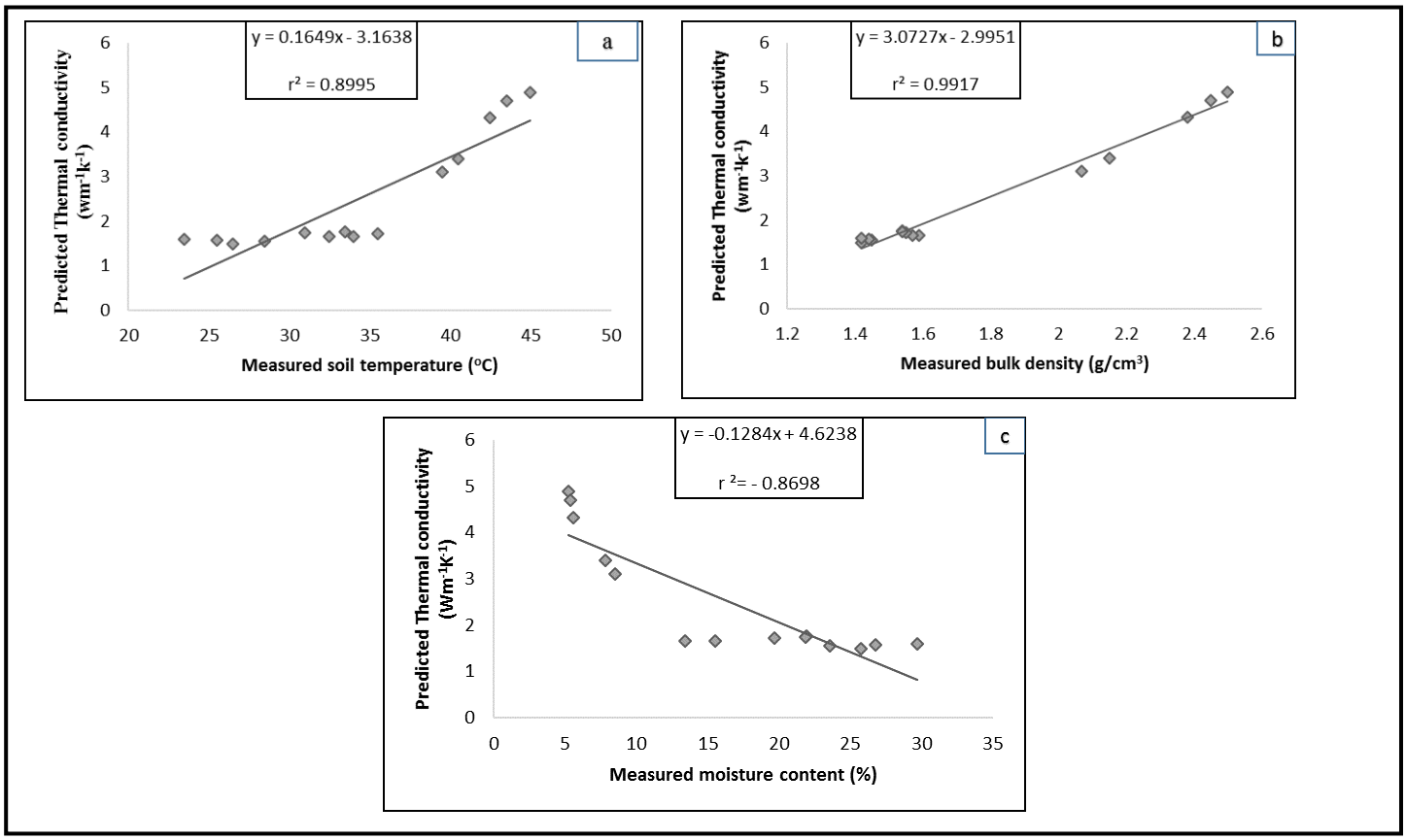


Fig. 3: Relationship between predicted soil thermal conductivity and (a) measured soil temperature; (b) measured bulk density and (c) measured moisture content at 0 – 30 cm sampling depth.

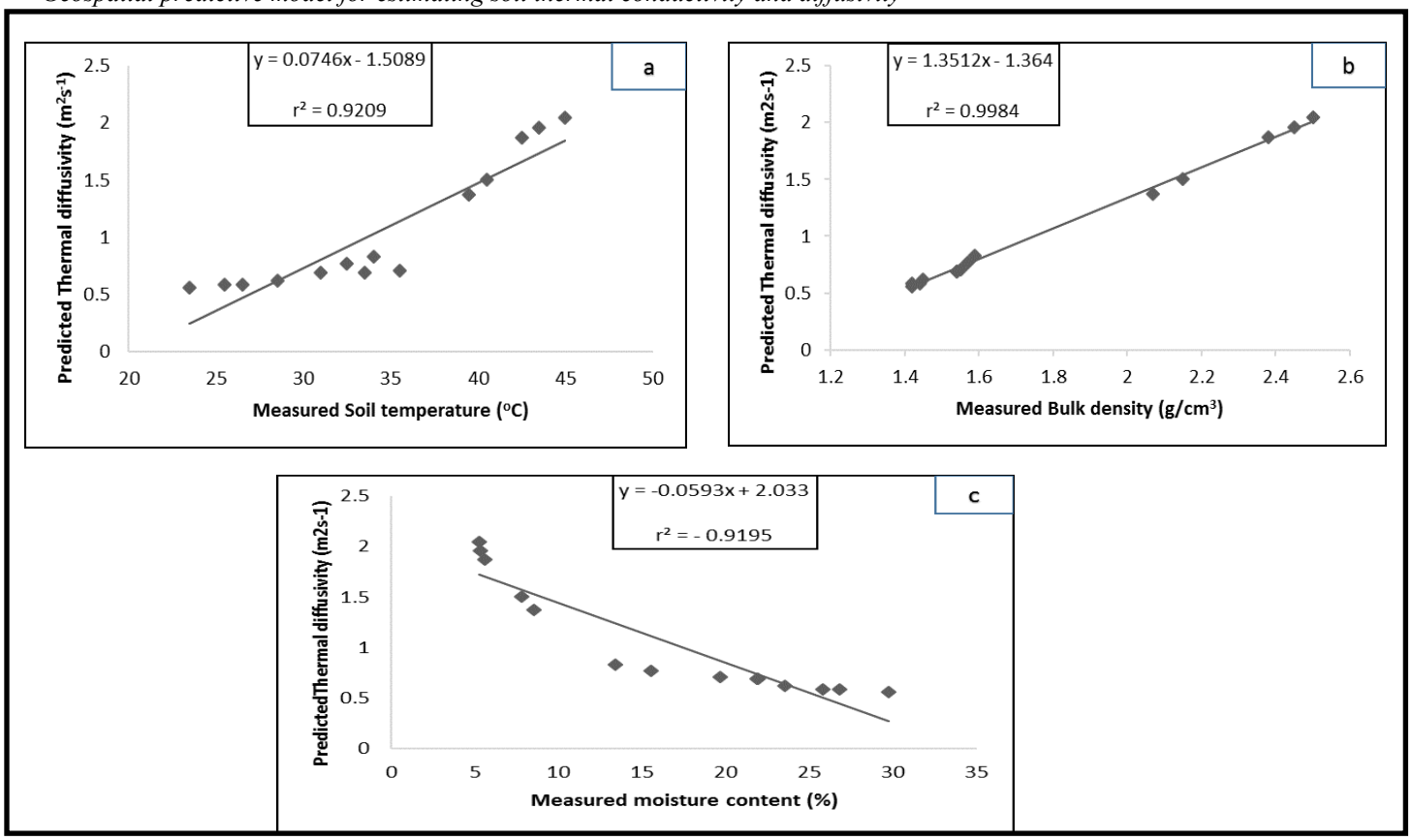


Fig. 4: Relation between predicted soil thermal diffusivity and (a) measured soil temperature; (b) measured bulk density and (c) measured moisture content respectively at 0 – 30 cm sampling depth.

(1994) and Smits *et al.* (2013).

3.2 Comparison of predicted conductivity and diffusivity values with selected measured soil properties

Relationships between predicted soil thermal conductivity values and measured soil temperature, bulk density and moisture content are shown in Figure 3a, 3b and 3c, respectively. There was a significant positive correlation for the relationship between predicted soil thermal conductivity with measured soil temperature and bulk density with r^2 value 0.89 and 0.99, respectively. That is, an increase in soil temperature and bulk density resulted in a corresponding increase in predicted soil thermal conductivity from sample points closer to the flare station to points farther away. In contrast, the relationship with moisture content showed a negative correlation with high r^2 0.86 value, i.e. a decrease in moisture content increased predicted soil thermal conductivity.

Similarly, predicted soil thermal diffusivity was positively correlated for measured soil temperature and bulk density with r^2 values 0.92 and 0.99, respectively, unlike that of moisture content that was negatively correlated with r^2 value 0.92. This result for bulk density agreed with many authors (Oladunjoye and Sanuade, 2012; Rubio *et al.,* 2009; Singh and Devid, 2000), but not with moisture content. They stated that increased bulk density and moisture content results to increase in soil thermal conductivity. This could be attributed to the increased soil temperature and prolonged heat emission from the flare site, which could have resulted in high evaporation at closer sample points to the flare vicinity.

3.3 Predictive Kriged maps

The real output of the geostatistical process maps showing the spatial distribution of the measured soil properties. These maps, therefore, have higher than maps presented for mapping units which implies that detailed and precise observation can be made on the spatial distribution of soil properties especially the thermal properties that cannot be routinely determined in the laboratory. Cruz-Rodriguez (2004), in the agreement, stated that detailed observations could be made on the distribution of soil properties when considering land use.

3.4 Spatial distribution maps of soil temperature

The kriged spatial maps of measured soil temperature, predicted soil thermal conductivity and diffusivity from the horizontal gas flaring site are the main output of the geostatistical analysis, as shown in Figs. 5, 6 and 7. Regions in the map with darker colour represent zones with higher values whereas regions with lighter colour represent moderate to low values. From the GIS readings, the coordinates of the active point of the flare were situated north-west direction at $4^{o}\,58'\,47.35^{o}$N and $7^{o}\,10'\,58.45$ of the area. The spatial kriged map for soil temperature in both studied depths (0 – 15 cm and 15 – 30 cm) was characterized by positional similarity in parameter values concentrated in the north-west zone in the direction of the flaring. The concentration showed well pattern varying multi-region in both depths. Clearly, from the spatial map, the subsurface depth showed more uniformity in parameter

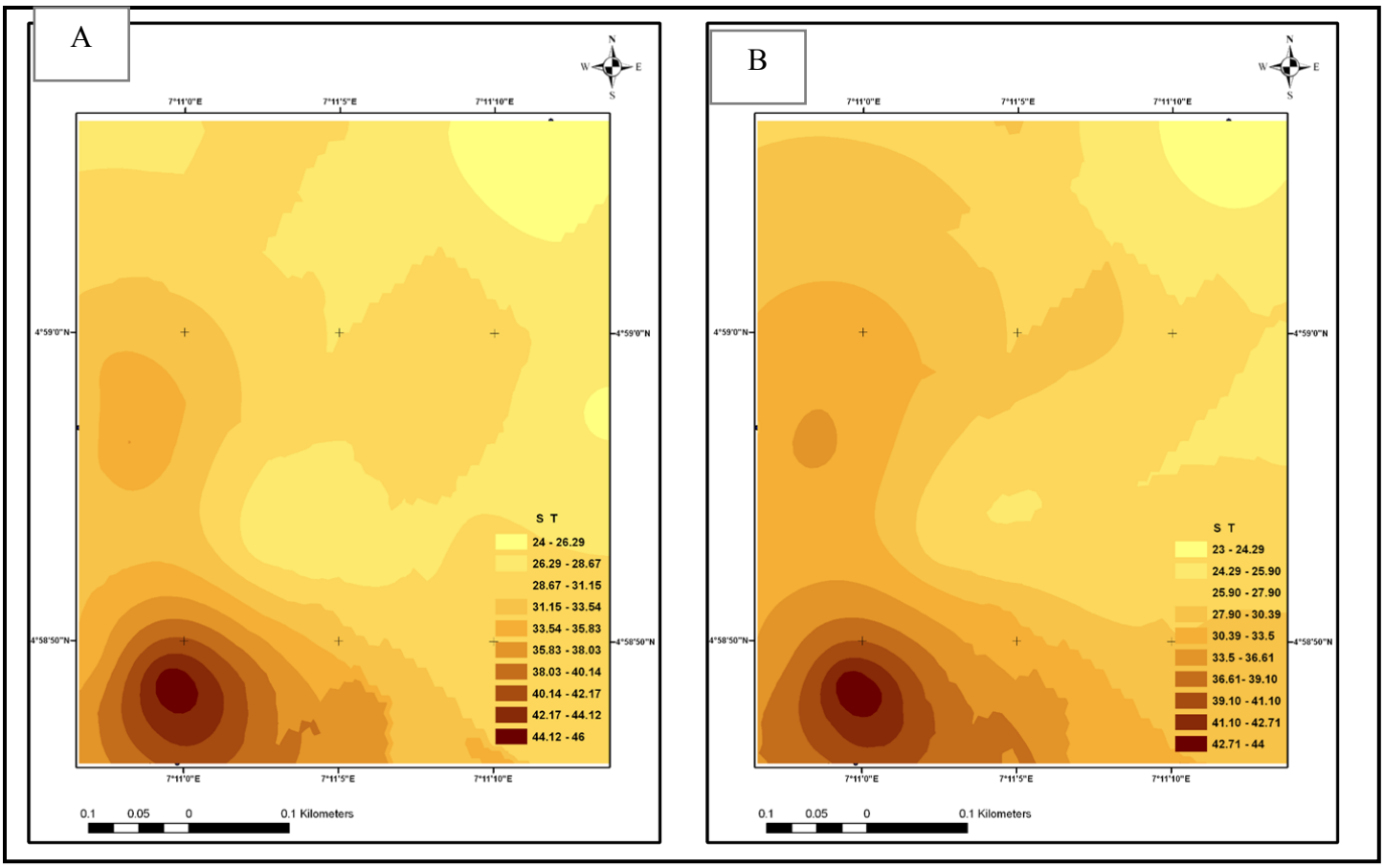


Figure 5: Spatial variability map of measured soil temperature at (a) surface soil (0 – 15 cm) and (b) subsoil (15 – 30 cm) at different distances away from the active flare point for rainy season observation.

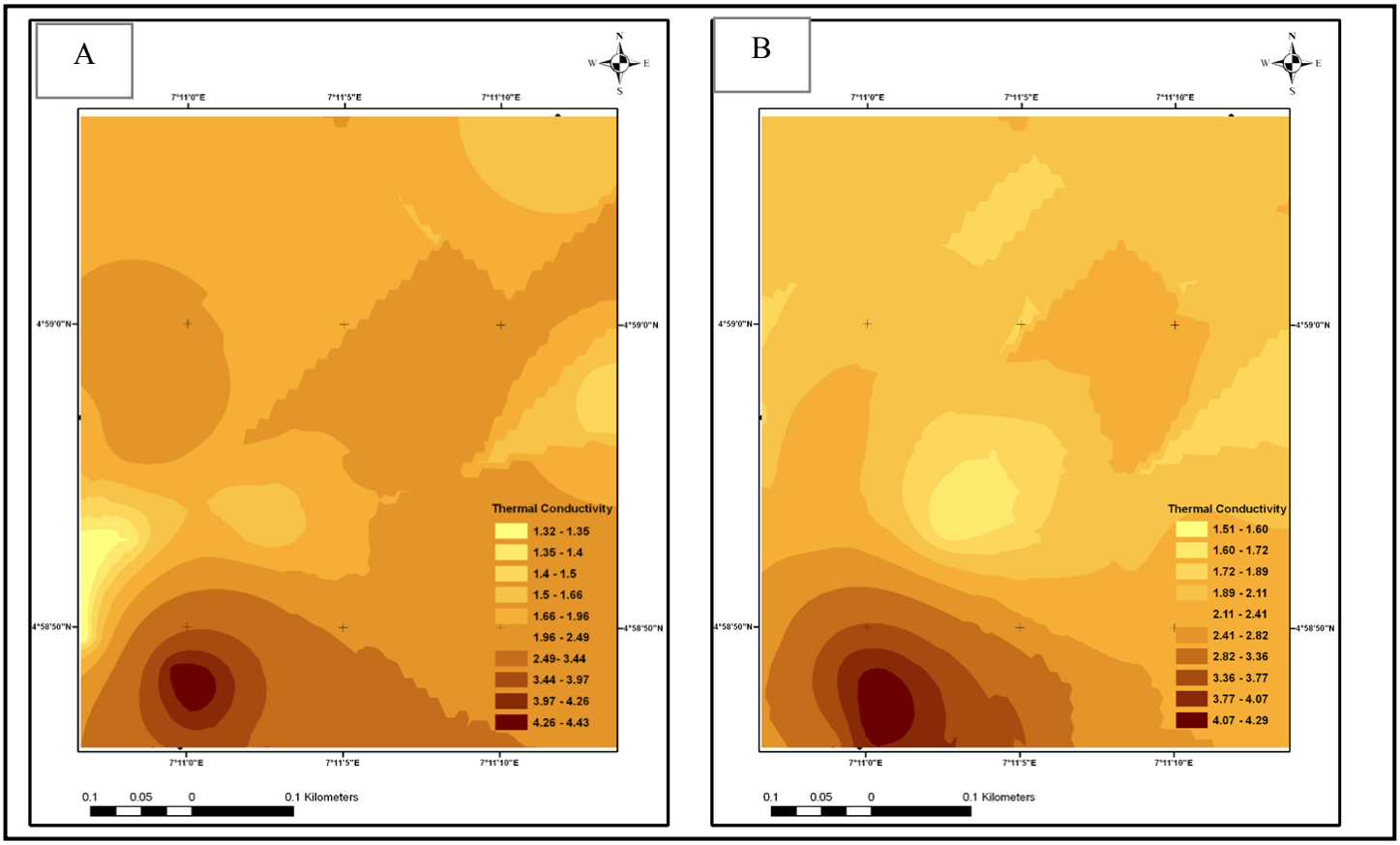


Figure 6: Spatial variability map of predicted soil thermal conductivity at (a) surface soil (0 – 15 cm) and (b) subsoil (15 – 30 cm) within varying distances away from active flare point for rainy season observation.

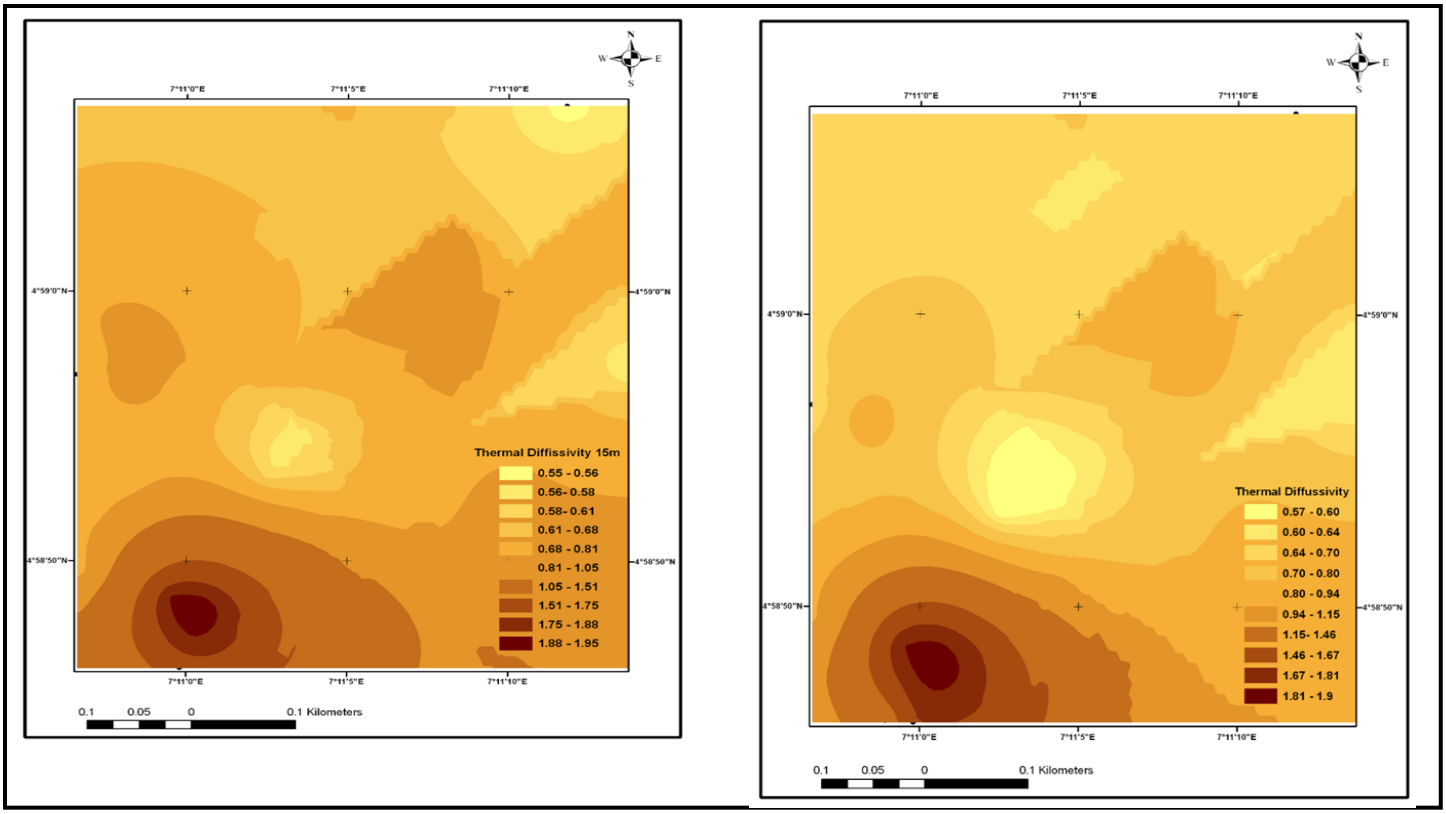


Figure 7: Spatial variability map of predicted soil thermal diffusivity at (a) surface soil (0 – 15 cm) and (b) subsoil (15 – 30 cm) within vaing distances away from the active flare point for rainy season observation.

distribution in the flare direction. Lower parameter values (28.67 – 24^{o}C) were observed in the southeastern, mid-east and north-eastern part of the area. It is evident from the spatial map that the subsurface depth (15 – 30 cm), experienced higher soil temperature spatial distribution (Figure 5). This agrees with the findings of many authors. Orubu (2002) observed that tremendous heat generated within the vicinity of gas flaring induces thermal pollution. Similarly, findings of Alakpodia (200) and Akpobome (2004) asserted that soils closer the flare sites are impoverished because the heat from the gas flare disturbs the process of eluviation and hydrolysis.

3.5 Spatial distribution maps of predicted soil thermal conductivity

From the kriged maps (Figure 6), the north western part of the site had predicted soil thermal conductivities in the range of 2.49 – 4.43 $Wm^{-1}K^{-1}$ in the surface depth (0 – 15 cm), however, the subsurface depth (15 – 30 cm) observed similar positional similarity as the surface depth as shown from the spatial map. But clearly, from the maps, the surface depth showed greater stretch in parameter distribution and uniformity in the north-western, south-eastern, mid-western and north-eastern unlike the subsurface depth that showed higher concentration in the north-west area with few patches at the mid-western and southern area of the spatial map (Figure 6). A general trend of increasing varying patterned predicted soil thermal conductivity values at decreased distances to the flare point were observed in both depths (Figure 6).The high spatial distribution of predicted soil thermal conductivity values in the surface depth could be attributed to the tremendous heat impact on the bare soil and subsequent transmission through the soil profile. This agrees with previous studies by Udoinyang (2005), that higher thermal conductivity values closer gas flare sites could be as a result of intense heat and higher temperature generated by the flare. Ikelegbe (1993) and Orubu (2002) observed that gas flaring generate tremendous heat, which is felt over an average radius of 0.5 kilometres thereby causing thermal pollution.

3.6 Spatial distribution maps of predicted soil thermal diffusivity

The pattern of the spatial distribution of predicted soil thermal diffusivity in both depths are displayed in Figure 7. From the spatial map, there was little dissimilarity in parameter values in both studied depths except that the surface (0 – 15 cm) depth observed uniform parameter distribution in the southeastern, mid-western areas of the site as evidenced in the spatial map. The lower parameter values (0.55 – 0.61 m^2s^{-1}) were found at the mid-eastern area to north-eastern in patches in both depths whereas the higher parameter values (1.51 – 1.98 m^2s^{-1}) in depths observed positional similarity of multi-region concentration to the north-west area of the site. From the spatial map, it can be observed that the surface (0 – 15 cm) depth showed more excellent spatial distribution and uniformity in the direction of the flare site. This could be as a result of high bulk density close to the flare vicinity due to the intense heat from the flare. Soils with high bulk density show massive structure, and less porosity and infiltration rate, hence, favouring high predicted thermal diffusivity of soils.

4. Conclusion

This study estimated the soil thermal conductivity and diffusivity at Owaza horizontal gas flaring site in Abia State,

Southeastern Nigeria using geostatistics. Geospatial characterization of spatial variability of predicted soil thermal properties via kriging showed rare insight into the way soil thermal properties within a horizontal gas flaring site vary. The highlighted results from the predictive model employed have shown that the predicted soil thermal properties varied in space and exhibited positional similarity in spatial patterns in the direction of the gas flare. The kriged maps for predicted soil thermal conductivity and diffusivity generated in the study suggest that no meaningful agricultural activity can thrive within the flare bond wall sample distances (sample points 1 through 7). This is attributable to the obvious scorched soils as a result of relatively high temperature values (32.5 – 45 ^{o}C) within the gas flare vicinity. Overall, the surface depth (0 – 15 cm) exhibited greater spatial distribution than the subsurface depth (15 - 30 cm). The predictive spatial maps generated could be a helpful tool to farmers, soil scientists, and other land users to make informed decisions on the appropriate distances and geographic direction for sustained use. A distance of at least 4 km away from a horizontal gas flare site is recommended for good soil physical characteristics.

References

Abu-Hamdeh, N.H. (2000). Effect of tillage treatments on soil thermal conductivity for some Jordanian clay loam and loam soils. *Soil Tillage Research*, 56, 145–151.

Abu-Hamdeh, N.H., and Reeder, R.C. (2000). Soil thermal conductivity: Effects of density, moisture, salt concentration, and organic matter. Soil Sci. Soc. Am. J., 64, 1285–1290.

Akpobome, C.A. (2004). Oil spillage and gas flaring and environmental degradation in the Niger Delta, Nigeria. *Journal of Environmental Analysis*, 2, 18–26.

Alakpodia, J. (2000). Soil Characteristics under Gas Flare in Niger Delta, Southern Nigeria Geo-Studies Forum. *Am Int. J. Environ, Policy* Issues, 1, 1-10.

APHA (1985). Standard Methods for the examination of wastewater, 15th ed. *American Public Health Association*, Washington DC.

Arocena, J. M. and Opio, C. (2003). Prescribed fire-induced changes in properties of sub-boreal forest soils. *Geoderma*, 113(1), 1-16.

Benka-Coker, M. O. and Ekundayo, J. A. (1997). Applicability of evaluating the ability of microbes isolated from an oil spill site to degrade oil. *Environmental Monitoring and Assessment, 45(3), 259-272.*

Blake G.R and Hartage K.H. (1990). Methods of soil analysis part and physical and mineralogical methods, 2nd edition. Madison. W.I ASA and SSSA, pp. 363-375. Agron. Monogram 9.

Botkin D.B and Keller E.A. (1995). Environmental Science: The Earth as a Living Planet-2nd Edition. John Wiley and Sons, Canada.

Botkin, D.B and Keller E.A. (1998). Environmental Science Earth as a Living Planet. 2nd Edition John Wiley and Sons, Canada.

Bouma, J. (1989). Using soil survey data for quantitative land evaluation. *Advances in Soil Science,* 9, 177–213.

Campbell, G.S. (1985). Soil physics with BASIC: Transport models for soil-plant systems. Elsevier, New York.

Campbell, G.S., Jungbauer, J.D., Bidlake, W.R. and Hungerford, R.D. (1994). Predicting the effect of temperature on soil thermal conductivity. *Soil Sci.,* 158, 307–313.

Chukwu, G.O. (2007). Soil Fertility Capability Classification for Seed Yam (*Dioscorea rotundata* Poir) on Acid Soils of South-Eastern Nigeria*, Unpublished PhD thesis* Submitted to Federal University of Technology, Minna, Niger State, Nigeria, pp. 190.

Cohen, J., Cohen, P., West, S. G., Aiken, L. S. (2013). Applied multiple regression/correlation analysis for the behavioural sciences. Routledge, New York.

Cruz, C. D. (2013). Genes: a software package for analysis in experimental statistics and quantitative genetics. Acta Scientiarum. *Agronomy,* 35(3), 271-276.

Cruz-Rodriguez, L. (2004). Soil organic carbon and nitrogen distribution in a tropical watershed. MSc. Thesis. University of Puerto Rico, Mayagüez campus.

Danelichen, V. H. M, and Biudes, M. S. (2011). Avaliação da Difusividade Térmica de um Solo no Norte do Pantanal. *Ciênciae Natura*, 33(8), 227-240.

Ekwue, E.I., Stone, R.J., Bhagwat, D. (2006). Thermal conductivity of some compacted Trinidadian soils as affected by peat content, *Biosystems Engineering*, 94, 461-469.

Ekwue, E.I., Stone, R.J., Bhagwat, D. (2011). Thermal conductivity of some common soils in Trinidad. *West Indian Journal of Engineering,* 33, 4 -11.

Ekwue, E.I., Stone, R.J., Maharaj, V.V., Bhagwat, D. (2005). Thermal conductivity and diffusivity of four Trinidadian soils as affected by peat content. *Transactions of the ASAE,* 57, 1803-1815.

Enwezor, W.O., Udo E.J., Ayorade, W.A., Adepuju, J. and Chude V.O. (1990). A Review of Soil and Fertilizer use Research in Nigeria. In: Literature Review on Soil Fertility Investigation in Nigeria. Federal Ministry of Agriculture and Natural Resources., Lagos, pp.53-100.

Gee, G.W., and Or, D. (2002). Particle-size analysis. In J.H. Dane and G.C. Topp (ed.) Methods of soil analysis. Part. 4. Physical methods. SSSA Book Ser. 5. SSSA, Madi-

son, WI., pp. 255–293.

Ghuman, B. S. and Lal R., 1985. Thermal conductivity, thermal diffusivity, and thermal capacity of some Nigerian soils. *Soil Science*, 139, 74–80.

Hassan, A. and Kouly, R., (2013). Gas flaring in Nigeria: Analysis of changes in its consequent carbon emission and reporting. *Accounting Forum,* 37(2), 124–134

Hewitt, D.N., Sturges, W.T. and Noah, A. (1995). Global Atmospheric Chemical Changes. Chapman and Hall Publishers New York.

Hillel, D. (1998). Environmental Soil Physics. Academic Press, London, pp. 771.

Hopmans, J.W., and Dane. J.H. (1986). Thermal conductivity of two porous media as a function of water content, temperature and density. *Soil Sci.,* 142, 187–195.

Ikelegbe, O. O. (1993). Pollution in Nigeria, cause, effect and control. 20th Proceeding of Nigeria Geographical Association Conference, Minna, Nigeria, pp. 17-18

Jang, H.D. (2004). Environment and crops. In: Uwehi, Z.S. (ed.). Principles of Environmental Management, Ibadan: ONAKS Press, pp. 106–30.

Lloyd, J. and Taylor, J. A. (1994). On the temperature-dependence of soil respiration. *Functional Ecology*, *8, 315–323.*

Luo, L. F., Robock, A., Vinnikov, K. Y., Schlosser, C. A., Slater, A. G., Boone, A., Braden, H., Cox, P., de Rosnay, P., Dickinson, R. E., Dai, Y. J., Duan, Q. Y., Etchevers, P., Henderson-Sellers, A., Gedney, N., Gusev, Y. M., Habets, F., Kim, J. W., Kowalczyk, E., Mitchell, K., Nasonova, O. N., Noilhan, J., Pitman, A. J., Schaake, J., Shmakin, A. B., Smirnova, T. G., Wetzel, P., Xue, Y. K. Yang, Z. L. and Zeng, Q. C. (2003). Effects of frozen soil on soil temperature, spring infiltration, and runoff: Results from the PILPS 2(d) experiment at Valdai, Russia. *Journal of Hydrometeorology,* 4, 334–351.

Nakshabandi, G.A. and Kohnke, H. (1965). Thermal conductivity and diffusivity of soils as related to moisture tension and other physical properties. *Agricultural. Meteorology*, *2*, 271–279.

Nelson, D.W. and Sommers, L.E. (1982). Total carbon, organic carbon, and organic matter. In: A.L. Page et al., editors, Methods of soil analysis. Part 2. 2nd ed. Agron. Monogr. 9. SSSA, and ASA, Madison, WI. pp. 539–579.

Noborio, K., McInnes, K.J. and Heilman. J. L. (1996). Two-dimensional model for water, heat, and solute transport in furrow-irrigated soil: II. Field evaluation. *Soil Science Society of American Journal,* 60, 1010–1021.

Odjugo, P.A.O. and Osemwenkhae, E.J. (2009). Natural gas flaring affects microclimate and reduces maize (Zea mays) yield. *International. Journal of Agricultural. Biology*, 11, 408–412

Oladunjoye, M. A. and Sanuade, O. A. (2012). In situ determination of thermal resistivity of soil: case study of Olorunsogo power plant, southwestern Nigeria. *International Journal of Recent Research and Applied Studies,* 13(2), 502–521.

Orubu, C. O. (2002). Oil Industry activities, Environmental Quality, and the Paradox of Poverty in Niger Delta. In: The Petroleum Industry, the Economy and the Niger-Delta Environment. (Eds), Orubu, C.O., Ogisi, D.O. and Okoh, R.N., pp. 17-31.

Rubio, M. C., Cobos, D. R., Josa R. and Ferrer, F. (2009). A new analytical laboratory procedure for determining the thermal properties in porous media, based on the American standard D5334-05, Estudios en la Zona no Saturada del Suelo IX 18-20.

Singh, D. N. and Devid, K. (2000). Generalized relationships for estimating soil thermal Resistivity. Experimental Thermal and Fluid Sciences, 22, 133-143.

Smits K.M., Sakaki T., Howington S.E., Peters J.F. and Illangasekare T.H. (2013). Temperature depend-ence of thermal properties of sands across a wide range of temperatures (30–70°C). *Vadose Zone Journal,* 12(1), 1-8.

Udoinyang, G.U. (2005). The effects of gas flaring on sweet potato production in the Niger Delta, Nigeria. *Journal of Ecosystem*, 10, 77–86.

USDA Soil Survey Staff (2003). Soil taxonomy: A basic system for making and interpreting soil surveys. 2nd ed. Agriculture Handbook 436, 128-129. Washington, D.C.: USDA.